

Mixed-Reference Spin-Flip Time-Dependent Density Functional Theory: Multireference Advantages with the Practicality of Linear Response Theory

Woojin Park, Konstantin Komarov, Seunghoon Lee,* and Cheol Ho Choi*



Cite This: *J. Phys. Chem. Lett.* 2023, 14, 8896–8908



Read Online

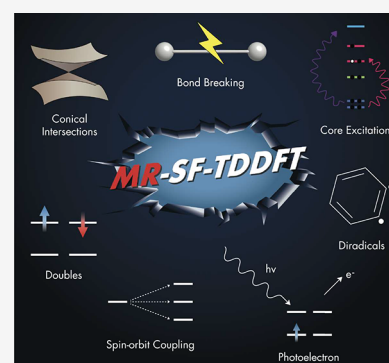
ACCESS |

Metrics & More

Article Recommendations

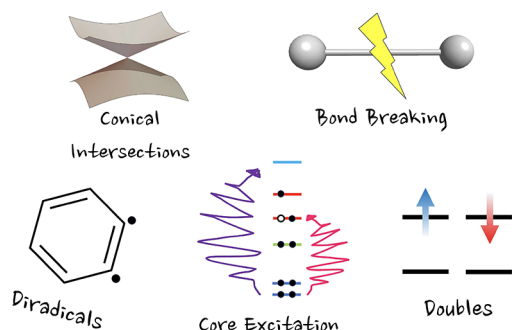
Supporting Information

ABSTRACT: The density functional theory (DFT) and linear response (LR) time-dependent (TD)-DFT are of the utmost importance for routine computations. However, the single reference formulation of DFT suffers in the description of open-shell singlet systems such as diradicals and bond-breaking. LR-TDDFT, on the other hand, finds difficulties in the modeling of conical intersections, doubly excited states, and core-level excitations. In this Perspective, we demonstrate that many of these limitations can be overcome by recently developed mixed-reference (MR) spin-flip (SF)-TDDFT, providing an alternative yet accurate route for such challenging situations. Empowered by the practicality of the LR formalism, it is anticipated that MRSF-TDDFT can become one of the major workhorses for general routine tasks.



One of the most challenging goals in electronic structure theory is to achieve a balanced description of *dynamical* and *nondynamical* (static) correlation effects in a cost-effective manner. Although density functional theory (DFT)¹ has been the most successful and popular methodology, it struggles to handle open-shell singlet cases such as diradicals and bond breaking due to its single-reference formulation (see Scheme 1).^{2,3} Multireference theories,⁴ on the other hand, are

Scheme 1. Challenging Cases for DFT and LR-TDDFT



specifically designed for *nondynamical* correlation, which is essential for electronically degenerate or near-degenerate situations not only of open-shell species but also of electronically excited states and conical intersections. However, its missing *dynamical* correlations necessitate additional calculations in the forms of either perturbations⁵ or configuration interactions,⁶ making the resulting theories impractical for large systems or

time-consuming tasks like nonadiabatic molecular dynamics (NAMD) simulations.⁷ In fact, our interest in the development of new quantum theories stems from the study of nonadiabatic processes.

In addition to the accurate descriptions of ground electronic states, proper and efficient quantum theories for strongly correlated excited states have become important as the demands for next-generation molecules and materials increase rapidly.^{8,9} Perhaps the most practical and popular methodology for studying the excited states is the spin-conserving linear-response time-dependent density functional theory (LR-TDDFT).^{10–12} It is based on the time-dependent Kohn–Sham (TD-KS) equation with the linear-response formalism using a closed-shell singlet ground state as its reference. Given a common set of reference orbitals (usually obtained by Kohn–Sham DFT), LR-TDDFT can conveniently produce a full spectrum of singly excited states in one calculation without any prior knowledge of the nature of states. Thus, it can easily access various properties, including excitation energies of all excited states, as well as interstate properties, like transition dipole moment (TDM), nonadiabatic coupling (NAC), spin–orbit coupling (SOC), core excitations, and so on. Despite all these advantages, there

Received: August 16, 2023

Accepted: September 21, 2023

Published: September 28, 2023



are well-known failures of this methodology, e.g., in describing the long-range charge transfer excitations,^{13–17} doubly excited states,^{18–20} bond breaking,^{21,22} and real and avoided conical intersections (CI) (see Scheme 1).^{23–26} To cope with some of these difficulties, DFT-based theories such as the state-specific orbital optimized (OO)-DFT methods have been actively developed,²⁷ featuring an unprecedented precision of DFT methods.²⁸ However, its state-specific orbital optimization requires prior knowledge of each state, which is not always straightforward.

In this regard, LR theories are still preferable because of their practicality and generality. Some of the drawbacks of TDDFT, in particular, the incorrect description of the conical intersections and the poor description of multireference electronic states, can be corrected by the spin-flip (SF)-TDDFT,^{29–31} as its open-shell high-spin triplet reference ($M_S = +1$) generates the ground singlet state as one of its response states as well as various configurations including important doubly excited ones (see Figure 1). However, the missing red configurations in Figure 1

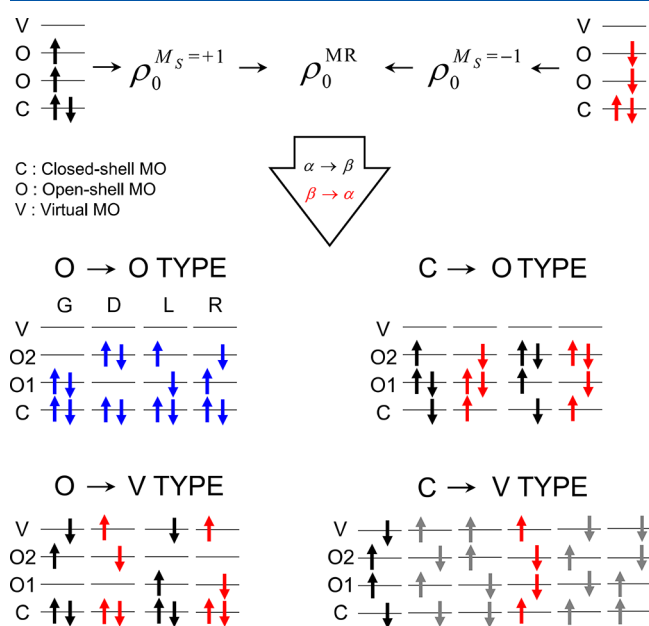


Figure 1. Upper panel shows the two references of MRSF-TDDFT denoted by black and red arrows. The zeroth-order MR-RDM which combines $M_S = +1$ and -1 RDMs is used in MRSF-TDDFT, while only the $M_S = +1$ RDM are used in SF-TDDFT. In the lower panel, the electronic configurations that can be generated by spin-flip linear responses from the MR-RDM are given by blue, black, and red arrows. The blue ones are generated from both references, which require a symmetrization procedure to eliminate OO-type spin contamination. The black and red ones are generated from $M_S = +1$ and -1 references, respectively. By contrast, those of SF-TDDFT are only the blue and black ones. Configurations that cannot be obtained even in MRSF-TDDFT are denoted by gray arrows.

inevitably introduce considerable spin contamination.^{32–34} Obviously, a fundamental solution to the problem is to recover the missing ones. However, unlike wave function theories, a significant challenge remains with respect to TDDFT when going beyond the adiabatic approximation to account for more than single excitations.³⁵ To alleviate the problem, the tensor equation-of-motion (TEOM) formalism was introduced yielding the spin-adapted (SA)-SF-DFT.³⁶ However, due to the

complexity of TEOM, its analytic energy gradient has yet to be derived.

Instead of introducing high-rank excitations from a single reference, a second red reference ($M_S = -1$) was introduced (see Figure 1) as an alternative way of expanding the response space by some of us.³⁷ In the realization of this idea, a new mixed reference state that has an equiensemble density of the $M_S = +1$ and $M_S = -1$ components of a triplet state was introduced:

$$\rho_0^{\text{MR}}(x) = \frac{1}{2} \{ \rho_0^{M_S=+1}(x) + \rho_0^{M_S=-1}(x) \} \quad (1)$$

The two references are transformed to a single *hypothetical* reference by the two spinor-like open-shell orbitals of s_1 and s_2 as shown in Figure 2a, whose one-particle reduced density matrix

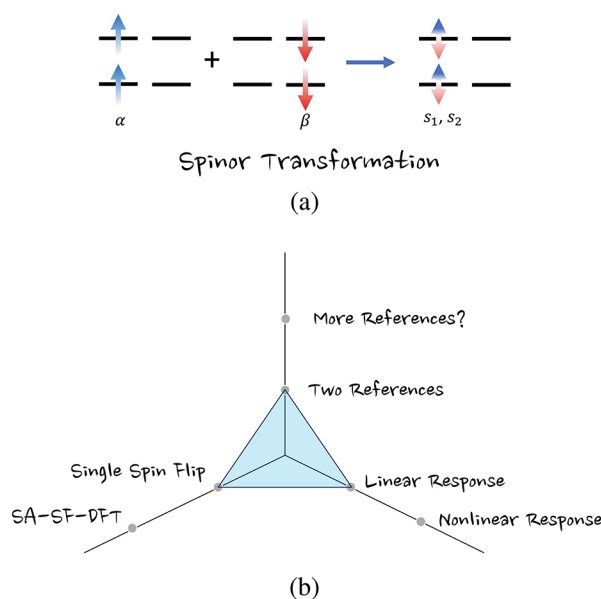


Figure 2. (a) The concept of spinor transformation, which combines two references into a single *hypothetical* reference. (b) The three axes of response theory, spin-flip idea, and multireference components, where the shaded area represents the MRSF-TDDFT.

(RDM) satisfies the *idempotent* condition. Finally, the linear response from the mixed *hypothetical* reference yields a mixed reference spin-flip (MRSF)-TDDFT.^{37,38} It is noted that the idea of two references is reminiscent of the multireference concept, although the exact formulations are fundamentally different. The immediate advantage of the new approach is the expanded response space without the expensive multireference orbital optimization, which profoundly affects its characteristics. To illustrate it, the major features of MRSF-TDDFT are first summarized in the following.

(1) Within the Tamm–Dancoff approximation,³⁹ the use of mixed-reference (MR)-RDM in the linear-response formalism yields two completely decoupled linear-response equations for the singlet and the triplet excited states, respectively³⁷

$$\sum_{rs} (A_{pq,rs}^{(k)(0)} + A_{pq,rs}'^{(k)}) X_{rs}^{(k)} = \Omega_{(k)} X_{pq}^{(k)}, \quad k = S, T \quad (2)$$

where $k = S, T$ represent singlet and triplet states, $A_{pq,rs}^{(k)(0)}$ is the orbital Hessian matrix, and $A_{pq,rs}'^{(k)}$ is a coupling matrix between the configurations originating from different components ($M_S = +1$ and $M_S = -1$).^{37,38} The remaining $X_{pq}^{(k)}$ and $\Omega_{(k)}$ are the amplitudes and excitation energies, respectively. The decoupled

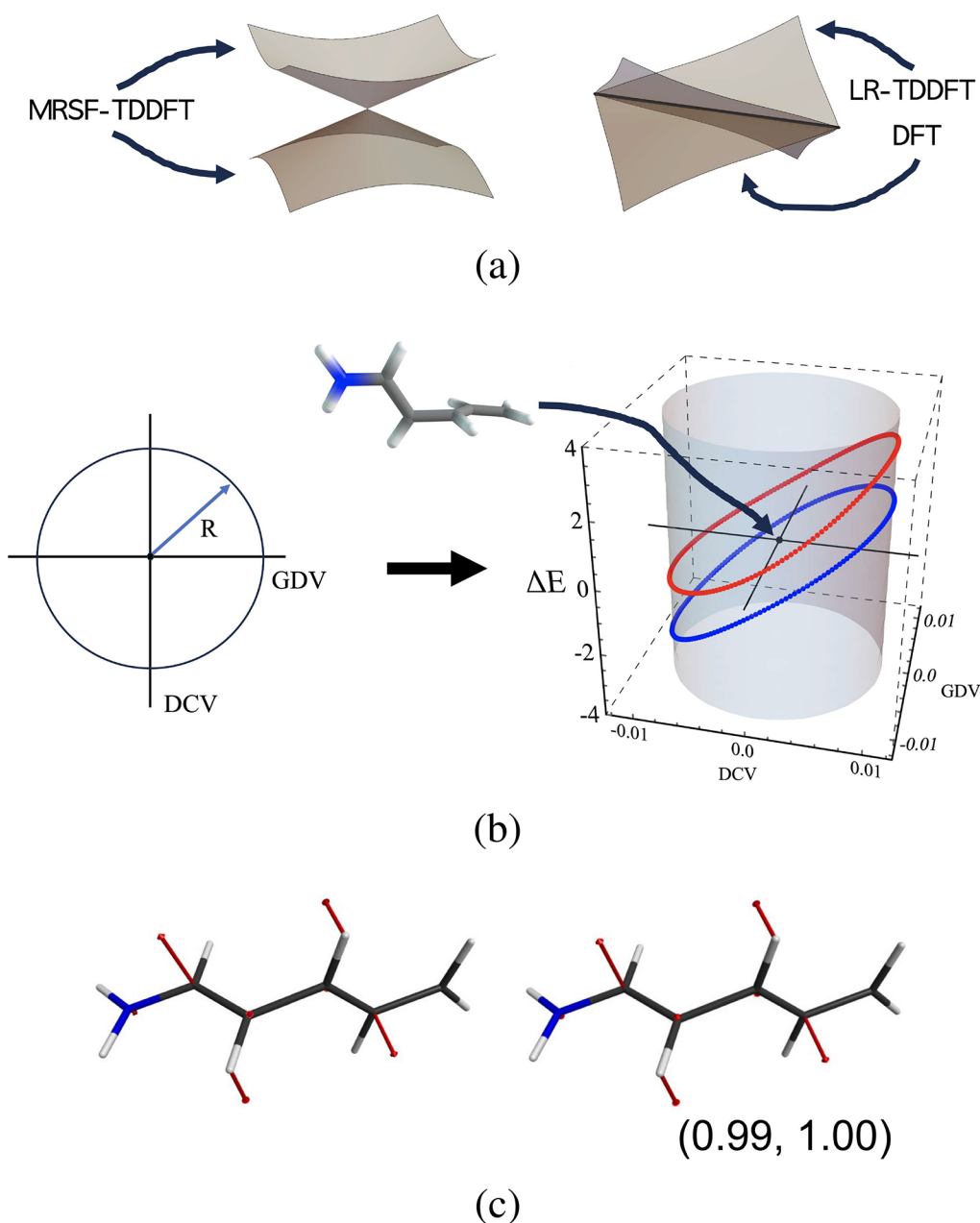


Figure 3. (a) The characteristic topology of the conical intersection (left) and linear intersection (right) between two potential energy surfaces of the S_1 and S_0 states. While MRSF-TDDFT can calculate both states, the combination of LR-TDDFT and DFT is needed for them. (b) The S_1 (red) and S_0 (blue) energies of CI_{tw-BLA} of trans-penta-2,4-dieniminium cation (PSB3) were calculated around a loop with the radius of 0.01 Å.⁴¹ The branching plane vectors were calculated using the algorithm by Maeda et al.,⁴⁷ which yields orthogonal GDV and DCV. (c) NAC vectors (or DCVs) at the MECI geometries of PSB3, where the left and right images are obtained by MRCISD and MRSF-TDDFT/BH&HLYP, respectively.³ The MECI geometries were optimized by MRCISD in ref 48. The numbers in parentheses display the inner products between the MRSF and the MRCISD NAC vectors and the ratio $|NAC_{MRSF}|/|NAC_{MRCISD}|$ of the norms of the NAC vectors, respectively.

equations of eq 2 nearly eliminate the spin-contamination of SF-TDDFT. Correspondingly, the ambiguity with cumbersome spin-state identification is no longer needed. Therefore, MRSF-TDDFT can be readily applied to “black-box” type applications, such as geometry optimization, conical intersection search, and molecular dynamics simulations. Currently, the spin-flip excitations also generate configurations for quintet states. However, as they are not sufficiently generated, further developments are needed for the more accurate descriptions of quintet states.

(2) It should be noted that the triplet response states from eq 2 are the triplet states with $M_S = 0$, which is different from the high spin reference triplet ($M_S = +1$) of MRSF-TDDFT. Although they resemble each other, the former and latter are obtained by response and variational calculations, respectively. As the latter reference triplet does not have any couplings with other response states, it is logical and recommended that it should not be utilized together with response states and the lowest response triplet should be used instead. This practice is different from LR-TDDFT, where the reference ground singlet state has to be utilized.

(3) Both SF- and MRSF-TDDFT remarkably produce the ground singlet (S_0) state as one of their response states, different from LR-TDDFT. It allows a way of generating the multi-configurational ground singlet state, overcoming the single reference limitations of the DFT. Thus, both theories can describe the open-shell singlet such as diradicals,⁴⁰ as well as bond-breakings.³ The $O \rightarrow O$ type configurations in Figure 1, which include the **G**, **D**, **L** and **R** configurations with blue arrows, are mostly responsible for them. In particular, the $\alpha(O1) \rightarrow \beta(O1)$ and $\alpha(O2) \rightarrow \beta(O2)$ spin-flip transitions yield the **L** and **R** configurations, respectively. As the two configurations occur from the two distinct spin-flip transitions, their contributions to the final response state of SF-TDDFT may become unequal, which yields substantial spin-contamination. This problem was resolved in MRSF-TDDFT by averaging contributions of the same configuration originating from the different spin-flip orbital transitions from the two components, $M_S = +1$ and $M_S = -1$, of the MR state.³⁷

(4) The ability to generate the ground singlet state (S_0) by MRSF-TDDFT also resolves the topological conical intersection problem of LR-TDDFT⁴¹ as both S_0 and S_1 are in the same response states (see Figure 3a). On the other hand, the combination of DFT and LR-TDDFT has to be utilized in the case of LR-TDDFT, which does not guarantee correct state couplings. Further discussions can be found later in the main text.

(5) The simple one-electron spin-flip excitation from the mixed triplet reference produces not only *singly* but also various *doubly* excited configurations as shown in Figure 1 (with respect to the closed-shell configuration).⁴² The doubles are critical components for the accurate descriptions of excited states, bond breakings, conical intersections, etc., which significantly expands the applicability of MRSF-TDDFT.

(6) Recently, it has been demonstrated that the high spin triplet reference of MRSF-TDDFT provides a simple way of ensuring core-hole relaxation for accurate XAS (X-ray absorption),⁴³ which has been one of the main difficulties of LR-TDDFT. Detailed discussions can be found later in the main text.

(7) Conceptually, MRSF-TDDFT introduced one more axis (middle vertical line) of the multireference concept to the existing response theory and spin-flip operator axes as shown in Figure 2b. As a result, MRSF-TDDFT can take advantage of multireference and the practicality of linear response theory at the same time with the formal $O(N^4)$ scaling (practically it can be below $O(N^3)$ due to the integral screenings).⁴⁴ Although it is possible to further develop theories along other axes, such as nonlinear response theory or double spin-flip theory, the mixed-reference concept of MRSF-TDDFT appears to be the most practical and efficient way of introducing additional *explicit* electron correlations without sacrificing performance. The major computational bottlenecks of the response parts are the Davidson iterations,⁴⁵ which typically are computationally less demanding than the SCF parts in the case of response theory. Therefore, the MRSF-TDDFT does not add too much extra computational overhead to ground-state DFT calculations, a great practical feature for correlated theories. In a preliminary benchmark with our new quantum code,⁴⁶ the response part (Davidson iteration) took much less time than SCF as shown in Figure S1a, and the timing ratio of response/SCF in Figure S1b is on average 0.232.

(8) It is noteworthy that not all of the electronic configurations shown in Figure 1 can be recovered. In fact,

four out of six type $C \rightarrow V$ configurations (i.e., those shown by the gray arrows) remain unaccounted for. Typically, these configurations represent high-lying excited states and make insignificant contributions to the low-lying states of organic molecules.³⁷ Thus, the effect of the missing configurations on the spin contamination is expected to be small.

Overall, MRSF-TDDFT introduces *explicit* correlations to the *implicit* accounts of exchange–correlation functionals of DFT, attempting to balance the *dynamical* and *nondynamical* electron correlations. To showcase the above-mentioned formal advantages, selective studies done by MRSF-TDDFT are presented below.

Perhaps, one of the most challenging electronic structure issues is the correct description of conical intersections (CIs) as shown in Figure 3a.^{49,50} CIs are special geometries at which two (or more) adiabatic electronic states become degenerate,^{51–54} which provide efficient pathways for nonadiabatic population transfer.^{49,50,55–59} The degeneracy of the intersection is lifted along two unique directions,^{54,60,61} which are defined by the gradient difference (**g**) and derivative coupling (**h**) vectors (GDV and DCV, respectively) given by

$$\mathbf{g} = \frac{1}{2}(\nabla_{\mathbf{Q}} E_{S_1} - \nabla_{\mathbf{Q}} E_{S_0}) \quad (3a)$$

$$\mathbf{h} = \langle \Psi_{S_1} | \nabla_{\mathbf{Q}} | \Psi_{S_0} \rangle \quad (3b)$$

for the case of a crossing between the ground (S_0) and lowest excited S_1 singlet states. The most significant requirement for quantum mechanical theories to describe CIs is that it should produce nonvanishing nonadiabatic coupling between the intersecting states. Surprisingly, this requirement for the S_1/S_0 CIs is violated by most of the single-reference theories as well as some multireference theories, such as single-state (SS)-CASPT2.^{25,48,62} Multi-state multireference computational methods^{63–67} are capable of producing the correct topology of CIs,^{25,55,68,69} however at the expense of very high cost of computations. The popular LR-TDDFT methodology^{12,70,71} fails to yield the correct dimensionality of the S_1/S_0 CI seam and predicts a linear crossing instead^{23,25,72} (see the right panel of Figure 3a) as they have to be computed by independent DFT and TDDFT theories, respectively.^{23,25,72} Consequently, the absence of couplings between S_0 and its excited states would introduce significant uncertainties in the description of $S_1 \rightarrow S_0$ internal conversion processes.

In contrast, it is remarkable that MRSF-TDDFT is capable of producing the correct double-cone topology, as the spin-flip excitation from a triplet produces both S_1 and S_0 as its response states. The correct CI topology by MRSF-TDDFT method was demonstrated in a conical intersection of trans-penta-2,4-dieniminium cation (PSB3) (see Figure 3b), where the nonzero energy differences between the red (S_1) and blue (S_0) loops as calculated along the circle around the CI with the radius R ensure the conical topology.⁴¹ The full NAC vectors at the CI of PSB3 were also presented in Figure 3c, where the left and right images are obtained by MRCISD and MRSF-TDDFT/BH&HLYP, respectively. The numbers in parentheses display the inner products between the MRSF-TDDFT and the MRCISD NAC vectors and the ratio $|\text{NAC}_{\text{MRSF}}|/|\text{NAC}_{\text{MRCISD}}|$ of the norms of the NAC vectors, respectively. The two numbers with near unity emphasize the accuracy of NAC vectors by MRSF-TDDFT. Therefore, MRSF-TDDFT can produce not only the correct topology of CIs but also accurate NAC vectors. In a benchmark with 12 conical intersections, the relative

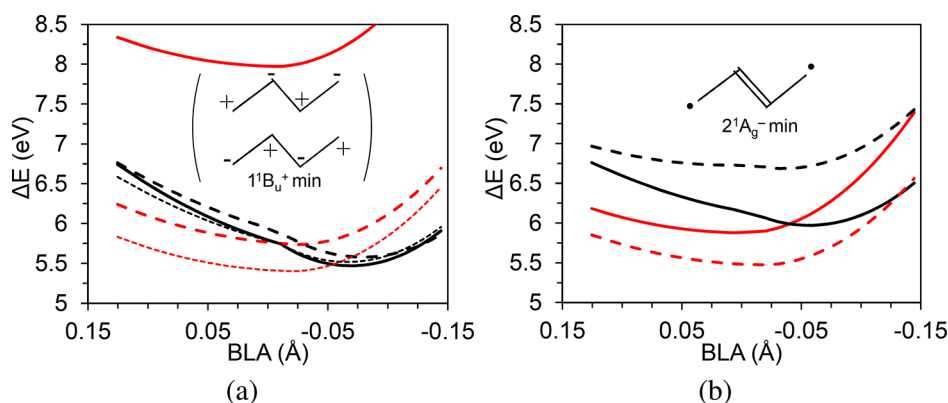


Figure 4. $1^1B_u^+$ (red) and $2^1A_g^-$ (black) energy profiles along the minimum-energy paths (MEPs) of *trans*-butadiene by (a) SA-CASSCF(4,4) (solid lines), δ -CR-EOMCC(2,3) (dashed lines), and XMS-CASPT2(4,4) (dotted lines). (b) The MEPs by MRSF/BH&HLYP (solid lines) and TDDFT/B3LYP (dashed lines). All calculations taken from ref 42 were done with cc-pVTZ. The BLA coordinate is defined as the difference between the average length of single bonds and the average length of double bonds.

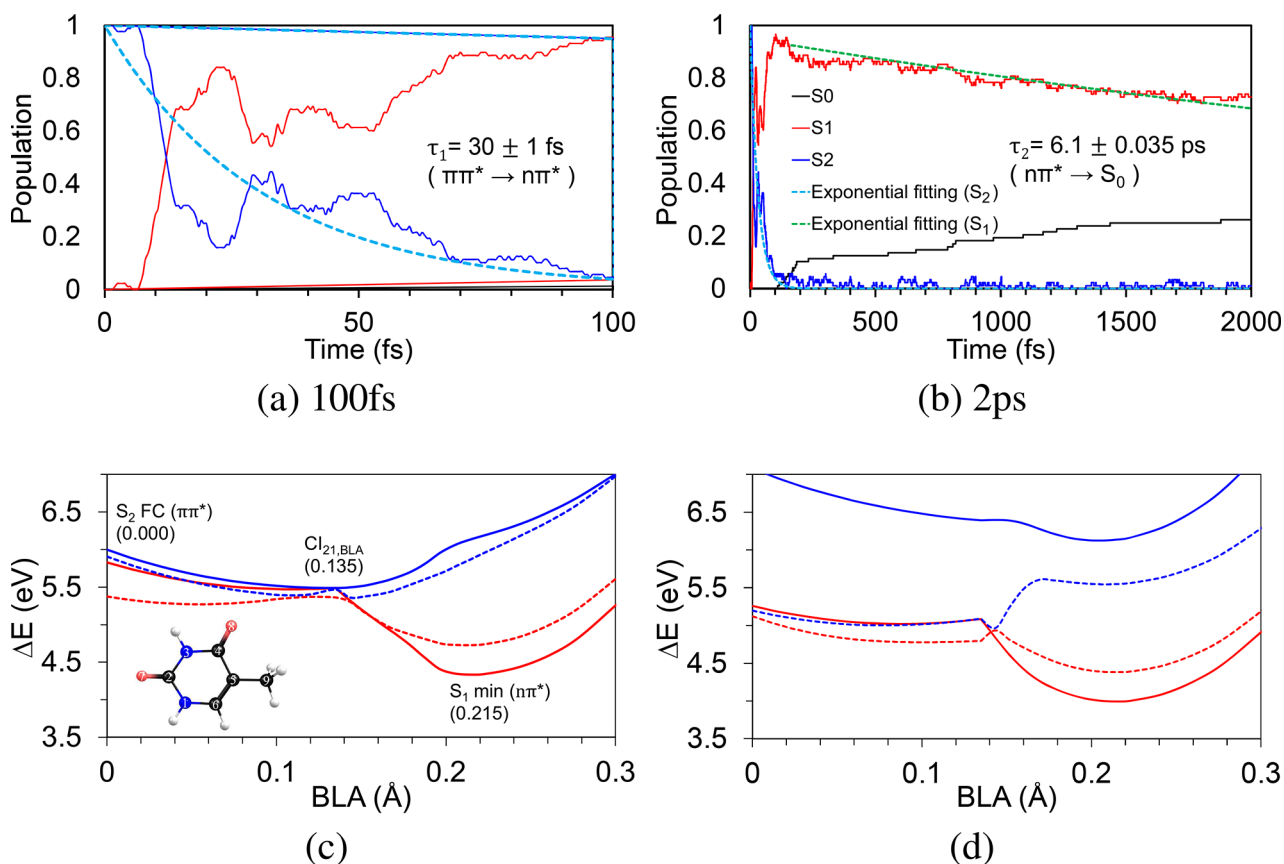


Figure 5. Time evolution of the adiabatic S_0 (black), S_1 (red), and S_2 (blue) populations for (a) the first 100 fs and (b) the entire 2 ps duration of the NAMD simulations taken from ref 86. The light blue curve in panel a and the green curve in panel b represent fittings of the S_2 and S_1 populations by a monoexponential function, respectively. Panel c compares the S_2 (blue) and S_1 (red) PES profiles along the MRSF MEPs (solid lines) with the EOM-CCSD curves (dashed lines). The molecular structure with atom numbers is given in the inset. Panel d shows the S_2 and S_1 PES profiles obtained with the 3SA-CASSCF(10,8) (solid lines) and the eXtended Multi-State Complete Active Space second-order Perturbation Theory (XMS-CASPT2, dashed lines). MEPs on the S_2 (blue) and S_1 (red) PESs optimized using the nudged elastic band (NEB)^{106,107} method in connection with MRSF-TDDFT and connecting the FC region, the $CI_{21,BLA}$, and the $S_{1,min}$ geometries; the respective BLA values are given parenthetically. The BLA coordinate is defined as the difference between the average increments of the lengths of the double bonds and the decrease of the single bond, $BLA = \frac{1}{2}(\Delta R_{C_4=O_8} + \Delta R_{C_5=C_6}) - \Delta R_{C_4-C_5}$, where ΔR 's are displacements with respect to the S_0 equilibrium geometry. For all other electronic structure methods, the MRSF-TDDFT MEP geometries are utilized by employing a 6-31G* basis set with Cs symmetry restriction. Adopted with permission from ref 84. Copyright 2009 American Chemical.

energies of CIs and their geometries by MRSF-TDDFT are in excellent agreement with those of MRCISD (RMSDs of 0.41 eV and 0.067 Å, respectively).^{41,73}

It has been shown that the nature of conical intersections among excited states (S_x , $x \geq 1$) are also strongly dependent on the quality of quantum mechanical theories even in the most

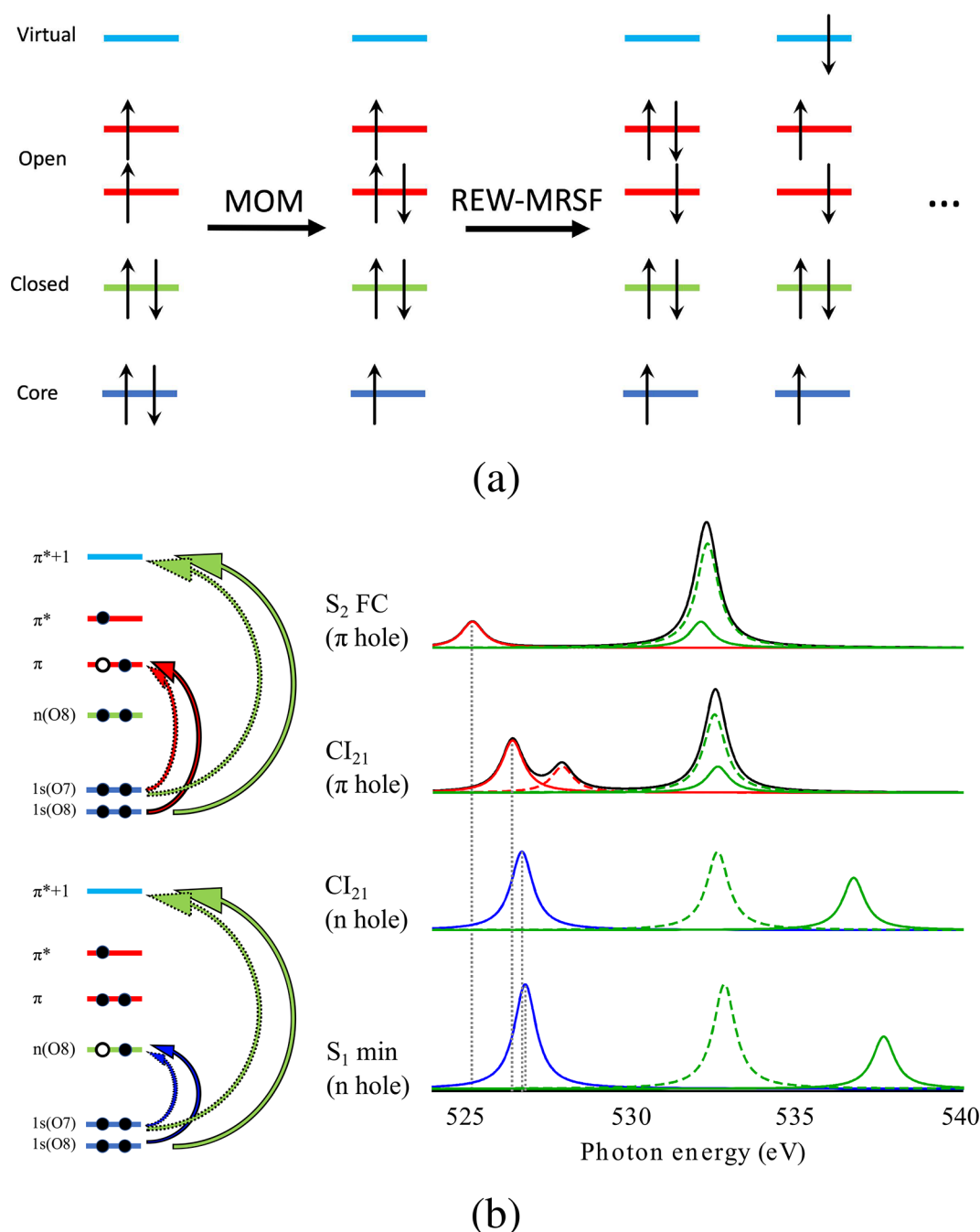


Figure 6. (a) The *core-hole relaxation* is accomplished by replacing the two singly occupied open (O1 and O2) orbitals of the ROHF reference with other ones. While the O1 is replaced with 1s, the O2 can be (a) the original LUMO orbitals. (b) The simulated *core to valence hole* spectra without an empirical shift and corresponding orbital transition diagrams of valence excited states of thymine by Δ CHP-MRSF(R)/BH&HLYP with aug-pcX-2/aug-pcseg-1, where the π and n holes are represented by blank circles. Oscillator strengths for Δ CHP-MRSF(R) are taken from CHP-MRSF(R) results. The core to π , n , and $\pi^* + 1$ holes are represented by red, blue, and green colors. The solid and dotted lines represent the excitations from 1s(O8) and 1s(O7) core, respectively (see Figure S for atom numbering). Here, we introduce a *double hole particle* relaxation, which relaxes a core and a valence hole at the same time. For example, the final configuration of $1s^1n^2\pi^{*1}$, which is $1s \rightarrow n$ core excitation of $n_{O8}\pi^*$ state can be accomplished by the $\pi^* \rightarrow n$ response excitation from the reference *double hole particle* CHP configuration of $1s^1n^1\pi^{*2}$. Adopted from with permission from ref 43. Copyright 2022 American Chemical Society.

prototypical and simple conjugated systems of *s-trans*-butadiene and *s-trans*-hexatriene.⁴² The bright $1^1B_u^+$ state comprises a zwitterionic one-electron HOMO (π) \rightarrow LUMO (π^*) transition,^{74–78} while the dark $2^1A_g^-$ state^{79–82} is dominated by multiconfigurations of the HOMO–1 \rightarrow LUMO and HOMO \rightarrow LUMO+1 one-electron and HOMO² \rightarrow LUMO² two-electron transitions. After the $\pi \rightarrow \pi^*$ transition to the bright

$1^1B_u^+$, the bond length alternation (BLA) motion along the geometric backbone leads to the conical intersection between $1^1B_u^+$ and $2^1A_g^-$.^{74–78,83–85} While high-level theories like δ -CR-EOMCC(2,3) and XMS-CASPT2 consistently predict that the $1^1B_u^+/2^1A_g^-$ crossing occurs near -0.03 Å along the BLA (dashed and dotted lines in Figure 4a, respectively), the corresponding potential energy surfaces obtained with SA-CASSCF (solid line

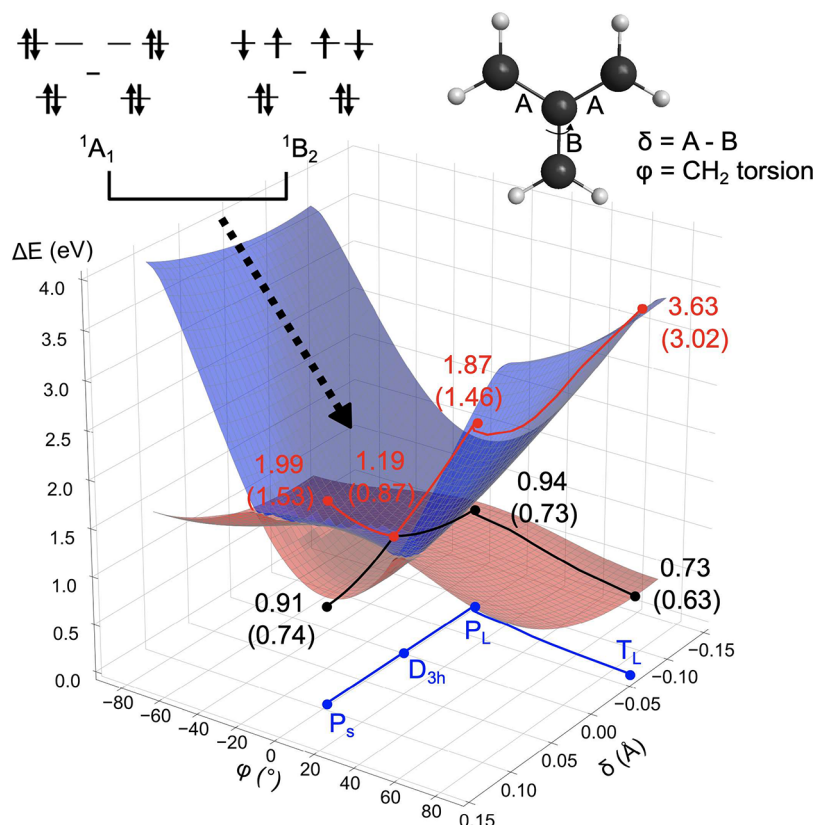


Figure 7. 3D potential energy surfaces of S_1 (red) and S_2 (blue) states around conical intersection (in D_{3h} system) between them. The energy paths that connect the stationary points on the lowest-energy triplet (blue) and two lowest-energy singlet (black and red) are shown in line. The triplet energy paths are projected on the bottom. The energies of MRSF-TDDFT and XMS-CASPT2 (in parentheses) are given next to the stationary points. The point with D_{3h} symmetry is marked as D_{3h} . The rest of the points have C_{2v} symmetry. ϕ is defined as the torsion angle of CH_2 while, δ is defined as the difference between two identical C–C bonds out of three (denoted as A) and the other bond (denoted as B). All data were taken from ref 40.

in Figure 4a) as well as with the LR-TDDFT (dashed line in Figure 4b) do not cross. The CASSCF misses the crossing by the overestimation of the zwitterionic $1^1B_u^+$ (red) state due to the missing *dynamical* electron correlation. On the other hand, TDDFT misses it, as the $2^1A_g^-$ (black) state near the CI region is not sufficiently stabilized due to the missing *doubly* excited configurations.⁴² Remarkably, MRSF-TDDFT (solid line in Figure 4b) properly recovers the crossing, as it can provide the *doubly* excited configurations to $2^1A_g^-$ (black).

As illustrated in the above examples, it is clear that MRSF-TDDFT can provide high-quality potential energy surfaces regarding conical intersections in part due to the balanced electron correlations, which is one of the most critical aspects for successful nonadiabatic molecular dynamics (NAMD) simulations. In the excited-state dynamics of thymine, the applicability of MRSF-TDDFT for the NAMD simulations was scrutinized.⁸⁶ Although theoretical simulations generally agree on the involvement of two excited states,^{87,88} namely, the optically bright S_2 state ($\pi \rightarrow \pi^*$) and the dark S_1 state ($n \rightarrow \pi^*$), its slow kinetics of the excited-state decay has been a subject of debate.^{89–100} As a result, three different decay mechanisms of S_1 -, S_2 -, and S_2 & S_1 -trapping¹⁰¹ models were theoretically proposed. It is interesting that the S_2 -trapping model was proposed by the studies with CASSCF.^{90,102,103} In contrast, MRSF-TDDFT yielded an S_1 -trapping process with the experimentally consistent two time constants of $\tau_1 = 30 \pm 1$ fs and $\tau_2 = 6.1 \pm 0.035$ ps,⁸⁶ where the former and latter correspond to fast $S_2 \rightarrow S_1$ internal conversion via the conical

intersection $\text{CI}_{21, \text{BLA}}$ and slow $S_1 \rightarrow S_0$ decay, respectively. The corresponding state population changes from NAMD simulations are shown in Figure 5a,b. The fast $S_2 \rightarrow S_1$ has been well supported by the time-resolved X-ray absorption ($\tau_1 = 60$ fs)¹⁰⁴ as well as the recent photoelectron spectroscopy ($\tau_1 = 37 \pm 1$ fs) studies,¹⁰⁵ while the latter slow time scale has been experimentally well-documented.^{91–100}

It was found that the discrepancies between CASSCF and MRSF-TDDFT in terms of decay mechanisms came from the differences in the description of the $\text{CI}_{21, \text{BLA}}$ conical intersection of $S_2 \rightarrow S_1$ internal conversion as shown in Figure 5c,d, where it is seen that the MRSF-TDDFT curves (solid curves in Figure 5c) are in good qualitative agreement with the EOM-CCSD method (dashed curves) in terms of curve crossing between the two excited states along the BLA coordinate. While the XMS-CASPT2 (dotted line in Figure 5d) methods also show the curve crossing at the $\text{CI}_{21, \text{BLA}}$, the lack of the *dynamical* electron correlation in CASSCF (solid line) significantly overestimates the bright S_2 state relative to the dark S_1 and leads to the absence of the S_2/S_1 crossing, resulting in a slow $S_2 \rightarrow S_1$ relaxation (the S_2 -trapping model).

Thus, the NAMD study on thymine again revealed the importance of balanced *dynamical* and *nondynamical* electron correlations for successful excited-state simulations and its direct connection to the quality of inherent conical intersections.⁸⁶ At the same time, it is observed that the NAMD simulations in combination with MRSF-TDDFT can provide consistent results with experiments. The same techniques have also been applied

to other systems. In the case of uracil, a plausible photohydration mechanism was established by the newly discovered high-energy intermediate.¹⁰⁸ The ultrafast aromatization dynamics in the excited state were found in dihydroazulene by revealing a characteristic damped bond-alternation motion.¹⁰⁹ A new singlet-to-singlet TADF (thermally activated delayed fluorescence) was suggested on the basis of ultrafast equilibrium by excited-state dual minima.¹¹⁰ Equipped with practicality and accuracy, therefore, it is expected that the MRSF-TDDFT can become a *de facto* standard for excited-state nonadiabatic dynamics.

As mentioned earlier, the high spin triplet reference of MRSF-TDDFT provides a natural way of introducing core-hole relaxation effects as shown in Figure 6a,⁴³ where the core-hole is kept by maximum overlap method during ROHF process.¹¹¹ In the case of LR-TDDFT, the corresponding accuracy is crude, with errors as large as ~ 10 eV for second-period elements like C, N, O, and F,¹¹² and even larger errors for heavier elements. With the additional scalar relativistic effects on K-edge excitation energies of 24 s- and 17 third-row molecules, on the other hand, the particular Δ CHP-MRSF(R) exhibited near-perfect predictions with root-mean-square error (RMSE) ≈ 0.5 eV, featuring a median of 0.3 and an interquartile range of 0.4.⁴³ The XAS of valence excited states can also be calculated by the same protocol. The 1s core excitation spectra of oxygens either of $\pi\pi^*$ (π hole) and $n\pi^*$ (n hole) states of the three particular structures (FC, CI₂₁, and S_{1,min}) of thymine were simulated by Δ CHP-MRSF(R), and the results are presented in Figure 6b.⁴³ Remarkably, a near perfect 1s(O8) \rightarrow n(O8) core to valence n hole excitation value of 526.8 eV (exp. 526.4 eV) at S_{1,min} in the case of the aforementioned thymine is predicted without any empirical shift, supporting the experimental assignment.¹⁰⁴ Overall, MRSF-TDDFT is accurate enough to provide the reference values for the correct assignment of XAS peaks.

As KS DFT is based on a single reference, it finds difficulties in describing open-shell singlet systems such as diradicals as well as Jahn–Teller distortion phenomena. Diradicals are molecules with two unpaired electrons occupying two (nearly) degenerate molecular orbitals.^{113–119} As a result, the lowest singlet state requires open-shell treatment, which has been a major challenge for single-reference theories. When there is weak or no couplings between the two electrons, Hund's rule¹²⁰ dictates triplet ground state. As both singlet and triplet response states are described by $M_S = 0$ configurations in MRSF-TDDFT, the open-shell singlet (OSS) and triplet states can be well described by the two electronic configurations L and R shown in Figure 1. When the two unpaired electrons rather strongly interact¹²¹ with each other such as in diradicaloids, the OSS state is better approximated by a linear combination of two closed-shell configurations G and D with fractional weights.^{122,123}

As all the important configurations of L, R, G, and D as well as other configurations of Figure 1 can be adopted in the description of lowest OSS and triplet states, MRSF-TDDFT remarkably exhibited a high prediction accuracy of the adiabatic ST gaps as compared to available experimental values with the mean absolute error (MAE) of 0.14 eV.⁴⁰ In an application to the Jahn–Teller distortion of trimethylenemethane (TMM), MRSF-TDDFT also exhibited high accuracy. The TMM diradical has a triplet ground state, $^3A'_2$ and doubly degenerate $^1E''$ (1B and 1A states) singlets at the D_{3h} (C_2) symmetric geometry, where the 1B and 1A states are represented by the combination of L and R and the out-of-phase linear combination of the G and D configurations, respectively, as shown in Figure 7.

The degeneracy of the two singlet 1B and 1A states at D_{3h} symmetry is well predicted by MRSF-TDDFT, which is lifted by bond-length alternation geometric distortions (δ coordinate).⁵¹ Rotation along the dihedral angle φ , another Jahn–Teller distortion, leads to the lowest singlet state of the T_L geometry. The values of XMS-CASPT2 (numbers in parentheses) are generally in good agreement with MRSF-TDDFT, highlighting the quantitative accuracy of MRSF-TDDFT even in such a difficult multiconfigurational system.

The relativistic version of MRSF-TDDFT has also been developed considering the spin–orbit coupling (SOC) within the mean-field approximation,¹²⁴ which would be an ideal tool for the study of intersystem crossings of large systems. According to the benchmarks, the errors of $^3P_1 - ^3P_0$ splitting by SOC of C, Si, Ge, and Sn are less than 4% compared to experiments. The SOC values of 4-thiothymine by SOC-MRSF-TDDFT with various XC functionals are generally in excellent agreement with those of GMC-QDPT2 within ~ 10 cm^{−1}. Ionization potentials (IPs) and electron affinities (EAs) by MRSF-TDDFT were also realized with the help of extended Koopmann theory,¹²⁵ which is an essential technique for photoelectron spectroscopy as well as conceptualization of excited states by Dyson orbitals. The QM/MM embedding with the advanced electrostatic potential fitted (ESPF) method has been also established for the modeling of realistic systems or solvent effects.¹²⁶ The MRSF-TDDFT has finally been released publicly by the GAMESS (July 31, 2022 R1 Public Release Version).¹²⁷ A dedicated new software⁴⁶ for MRSF-TDDFT shall also be publicly released soon, which is ideally tuned for the best performance ($>10\times$ faster) of response theories.

In light of the aforementioned advantages, it is highly desirable to consider further developments and improvements of MRSF-TDDFT. As a variant of DFT, one of the real difficulties in the applications of MRSF-TDDFT is the choice of exchange–correlation (XC) functionals. They are approximate energy functionals, which are typically developed specifically for the ground state and therefore need not be successful in modeling the excited state. The collinear formulation of MRSF-TDDFT further limits the use of proper XC functionals, as only the exact exchange term survives.¹²⁸ As a result, XC functionals with a large contribution of exact exchange such as BH&HLYP with the economical 6-31G(d) or cc-pVDZ basis sets can be recommended for the most practical computations. The excitation energies are affected both by the reference KS orbitals and the elements of Casida A matrix or the orbital Hessian matrix. The former affects the HOMO–LUMO gaps mostly, while the latter determines the relative energies among response states. The large contribution of exact exchange in BH&HLYP tends to increase the HOMO–LUMO gap, and so do VEEs. Therefore, it would be interesting to see if effective density functionals explicitly designed for excited state or more preferably for MRSF-TDDFT can be developed. Regarding XC functionals, these approximate XC functionals in general do not exhibit the correct $1/r$ asymptotic behavior, where r is the electron–nucleus distance, but fall off too rapidly. Consequently, TDDFT in general gives substantial errors for excited states of molecules with extended π -systems as well as for charge-transfer (CT) states.^{13–17} Recently, by individually tuning XC functionals for SCF and response parts of computations, we have developed a new family of XC functionals designed for MRSF-TDDFT, which would alleviate these situations.¹²⁹ In the benchmarks against Thiel's set,¹³⁰ the conventional BH&HLYP functionals in combination with

MRSF-TDDFT exhibits the MAE = 0.379 eV and IQR = 0.511 eV, while the MAE of CC2 theory is 0.32 eV. However, the MAE by the recently developed new functionals of DTCAM-VEE is reduced to 0.218 eV and IQR = 0.327 eV, demonstrating the accuracy of VEE can be significantly improved. However, it should be emphasized that the VEEs are the properties of Franck–Condon geometries. The vast majority of potential energy surfaces including conical intersections are away from it, necessitating new strategies in the design of XC functionals for the excited state in general.

As illustrated in Figure 2b, it would be interesting to explore further expansion along the multireference axis, which would allow us to study even more difficult multiconfigurational systems such as metallic complexes with highly degenerated electronic states, where the response configurations generated by the current MRSF-TDDFT may not be sufficient. Methods for systems with odd electrons should be also developed. The idea of utilizing two references can be also applied to other theories such as the SF-Bethe–Salpeter equation (BSE) formalism of many-body perturbation theory,¹³¹ SF-algebraic diagrammatic construction (ADC),¹³² SF-ORMAS-CI (spin-flip occupation restricted multiple active space CI),¹³³ as well as SF-EOM-CC.¹³⁴ As MRSF-TDDFT can deal with strong correlations, its extension to solid systems can also be highly anticipated. In fact, we have shown that the quasi-particle approach on the basis of the extended Koopmann theorem can produce correlated band structures rather easily.¹³⁵

In summary, multiple benchmarks have established that the combination of the multireference concept with the linear response theory implemented in MRSF-TDDFT provides an efficient way of balancing the *dynamical* and *nondynamical* electron correlations, overcoming the major limitations of other quantum theories. In the current Perspective, the superior aspects of MRSF-TDDFT have been highlighted in the series of challenging applications such as conical intersections, non-adiabatic molecular dynamics (NAMD) simulations, core-hole relaxation, and diradicals. With its high performance, versatility, and practicality, it can be anticipated that MRSF-TDDFT will become one of the major workhorses for routine tasks of quantum chemical calculations. As its accuracy and capabilities can be further improved by developing specific XC functionals or expanding the response space, the future of MRSF-TDDFT and its variants is bright.

■ ASSOCIATED CONTENT

SI Supporting Information

The Supporting Information is available free of charge at <https://pubs.acs.org/doi/10.1021/acs.jpcllett.3c02296>.

A preliminary benchmark of MRSF-TDDFT performance (PDF)

■ AUTHOR INFORMATION

Corresponding Authors

Seunghoon Lee – Division of Chemistry and Chemical Engineering, California Institute of Technology, Pasadena, California 91125, United States; Present Address: Department of Chemistry, Seoul National University, Seoul 151-747, South Korea; orcid.org/0000-0003-3665-587X; Email: seunghoonlee@snu.ac.kr

Cheol Ho Choi – Department of Chemistry, Kyungpook National University, Daegu 41566, South Korea;

orcid.org/0000-0002-8757-1396; Email: cchoi@knu.ac.kr

Authors

Woojin Park – Department of Chemistry, Kyungpook National University, Daegu 41566, South Korea

Konstantin Komarov – Center for Quantum Dynamics, Pohang University of Science and Technology, Pohang 37673, South Korea

Complete contact information is available at: <https://pubs.acs.org/doi/10.1021/acs.jpcllett.3c02296>

Notes

The authors declare no competing financial interest.

Biographies

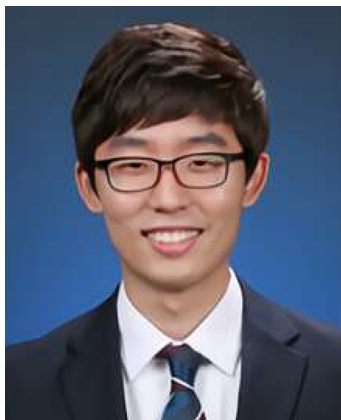


Woojin Park was born in Daegu, South Korea (1995) and received his B.Sc. and M.Sc. degrees in Chemistry from Kyungpook National University, where he worked in the group of Prof. Cheol Ho Choi. He is currently a Ph.D. candidate in the same group. He is interested in the development of quantum chemistry methods and their application to the exploration of chemical reactions in excited states, a field that is challenging to investigate experimentally. His particular focus is on the chemical reactions triggered by light absorption, followed by multiple subsequent processes such as vibrational relaxation, internal conversion, and intersystem crossing.

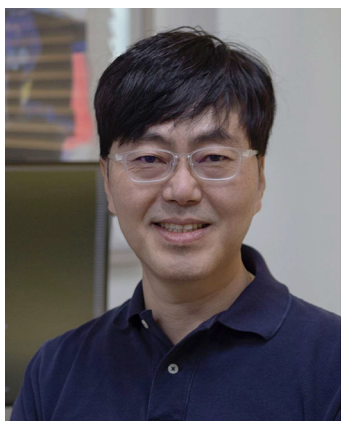


Konstantin Komarov, born in Krasnoyarsk, Russia, received a B.Sc. (2013) and a M.Sc. (2015) in Physics and a Ph.D. in Condensed Matter Physics (2021) from the Federal Research Center “Krasnoyarsk Science Center of the Siberian Branch of the Russian Academy of Sciences.” He is currently a postdoc at POSTECH University and has been working with Professor Cheol Ho Choi’s group at Kyungpook National University since 2021. His research focus revolves around enhancing

electronic structure methods for strongly correlated systems, with a particular emphasis on incorporating spin-orbit coupling effects.



Seunghoon Lee was born in Busan, South Korea (1989). He received his B.Sc. in Chemistry (2014) and Ph.D. in Physical Chemistry (2019) from Seoul National University in South Korea, supervised by professors Sangyoub Lee and Cheol Ho Choi. He has been a postdoc in professor Garnet K. Chan's group at Caltech since 2019. His research focuses on developing and improving electronic structure methods for strongly correlated systems, from diradicals to metal clusters.



Cheol Ho Choi was born in Daegu, South Korea (1967), and grew up in Daegu and Seoul, South Korea. He received B.Sc. and M.Sc. degrees in Chemistry from Seoul National University, South Korea, where he worked in the laboratory of Prof. Kwan Kim. In 1998, he obtained his Ph.D. (Hons) in Chemistry from Georgetown University, working with Prof. Miklos Kertesz. After postdoctoral research with Prof. Mark Gordon at Iowa State University, Choi started his independent career at the Kyungpook National University, Daegu, South Korea in 2001. He is currently Full Professor of Chemistry and the director of BK21 research center of the Chemistry Department. He is a Member of the American Chemical Society and the Korean Chemical Society and was awarded distinguished scholar from Kyungpook National University (2008), Young Physical Chemist (2009), and Ipjae Physical Chemist (2018) from the Korean Chemical Society. His research focuses on the development and application of efficient electronic structure methods and their applications especially on excited states.

■ ACKNOWLEDGMENTS

We are indebted to Prof. Klaus Ruedenberg, Prof. Mark Gordon, Dr. Mike Schmidt, Dr. Micheal Filatov, Dr. Miquel Huix-Rotllant, Dr. Hiroya Nakata, Prof. Piotr Piecuch, and Prof. Tao Tzeng for invaluable discussions and inspirations. This work was supported by the NRF funded by the Ministry of Science and ICT (2020R1A2C2008246 and 2020R1A5A1019141 to

C.H.C.) for the applications of developed theories. This work was supported by the National Supercomputing Center with supercomputing resources including technical support (KSC-2022-CRE-0353).

■ REFERENCES

- (1) Kohn, W.; Sham, L. J. Self-consistent equations including exchange and correlation effects. *Physical review* **1965**, *140*, A1133.
- (2) Squires, R. R.; Cramer, C. J. Electronic interactions in arylene biradicals. Ab initio calculations of the structures, thermochemical properties, and singlet-triplet splittings of the didehydronaphthalenes. *J. Phys. Chem. A* **1998**, *102*, 9072–9081.
- (3) Lee, S.; Horbatenko, Y.; Filatov, M.; Choi, C. H. Fast and Accurate Computation of Nonadiabatic Coupling Matrix Elements Using the Truncated Leibniz Formula and Mixed-Reference Spin-Flip Time-Dependent Density Functional Theory. *J. Phys. Chem. Lett.* **2021**, *12*, 4722–4728.
- (4) Schmidt, M. W.; Gordon, M. S. The construction and interpretation of MCSCF wavefunctions. *Annu. Rev. Phys. Chem.* **1998**, *49*, 233–266.
- (5) Battaglia, S.; Lindh, R. Extended dynamically weighted CASPT2: The best of two worlds. *J. Chem. Theory Comput.* **2020**, *16*, 1555–1567.
- (6) Werner, H.-J.; Knowles, P. J. An efficient internally contracted multiconfiguration-reference configuration interaction method. *J. Chem. Phys.* **1988**, *89*, 5803–5814.
- (7) Crespo-Otero, R.; Barbatti, M. Recent advances and perspectives on nonadiabatic mixed quantum-classical dynamics. *Chem. Rev.* **2018**, *118*, 7026–7068.
- (8) Hedley, G. J.; Ruseckas, A.; Samuel, I. D. Light harvesting for organic photovoltaics. *Chem. Rev.* **2017**, *117*, 796–837.
- (9) Endo, A.; Ogasawara, M.; Takahashi, A.; Yokoyama, D.; Kato, Y.; Adachi, C. Thermally activated delayed fluorescence from Sn^{4+} -porphyrin complexes and their application to organic light emitting diodes—A novel mechanism for electroluminescence. *Adv. Mater.* **2009**, *21*, 4802–4806.
- (10) Runge, E.; Gross, E. K. Density-functional theory for time-dependent systems. *Adv. Mater. Phys. Rev. Lett.* **1984**, *52*, 997.
- (11) Casida, M. E.; Chong, D. Recent advances in density functional methods. In *Computational Chemistry: Reviews of Current Trends*; 1995.
- (12) Casida, M. E.; Huix-Rotllant, M. Progress in time-dependent density-functional theory. *Annu. Rev. Phys. Chem.* **2012**, *63*, 287–323.
- (13) Dreuw, A.; Weisman, J. L.; Head-Gordon, M. Long-range charge-transfer excited states in time-dependent density functional theory require non-local exchange. *J. Chem. Phys.* **2003**, *119*, 2943–2946.
- (14) Dreuw, A.; Head-Gordon, M. Single-reference ab initio methods for the calculation of excited states of large molecules. *Chem. Rev.* **2005**, *105*, 4009–4037.
- (15) Dev, P.; Agrawal, S.; English, N. J. Determining the appropriate exchange-correlation functional for time-dependent density functional theory studies of charge-transfer excitations in organic dyes. *J. Chem. Phys.* **2012**, *136*, 224301.
- (16) Maitra, N. T. Undoing static correlation: Long-range charge transfer in time-dependent density-functional theory. *J. Chem. Phys.* **2005**, *122*, 234104.
- (17) Baerends, E.; Gritsenko, O.; Van Meer, R. The Kohn–Sham gap, the fundamental gap and the optical gap: the physical meaning of occupied and virtual Kohn–Sham orbital energies. *Phys. Chem. Chem. Phys.* **2013**, *15*, 16408–16425.
- (18) Cave, R. J.; Zhang, F.; Maitra, N. T.; Burke, K. A dressed TDDFT treatment of the 2^1A_g states of butadiene and hexatriene. *Chem. Phys. Lett.* **2004**, *389*, 39–42.
- (19) Neugebauer, J.; Baerends, E. J.; Nooijen, M. Vibronic coupling and double excitations in linear response time-dependent density functional calculations: Dipole-allowed states of N_2 . *J. Chem. Phys.* **2004**, *121*, 6155–6166.
- (20) Maitra, N. T.; Zhang, F.; Cave, R. J.; Burke, K. Double excitations within time-dependent density functional theory linear response. *J. Chem. Phys.* **2004**, *120*, S932–S937.

- (21) Aryasetiawan, F.; Gunnarsson, O.; Rubio, A. Excitation energies from time-dependent density-functional formalism for small systems. *EPL (Europhysics Letters)* **2002**, *57*, 683.
- (22) Filatov, M. Ensemble DFT approach to excited states of strongly correlated molecular systems. *Density-functional methods for excited states* **2015**, 368, 97–124.
- (23) Levine, B. G.; Ko, C.; Quenneville, J.; Martínez, T. J. Conical intersections and double excitations in time-dependent density functional theory. *Mol. Phys.* **2006**, *104*, 1039–1051.
- (24) Huix-Rotllant, M.; Filatov, M.; Gozem, S.; Schapiro, I.; Olivucci, M.; Ferré, N. Assessment of density functional theory for describing the correlation effects on the ground and excited state potential energy surfaces of a retinal chromophore model. *J. Chem. Theory Comput.* **2013**, *9*, 3917–3932.
- (25) Gozem, S.; Melaccio, F.; Valentini, A.; Filatov, M.; Huix-Rotllant, M.; Ferré, N.; Frutos, L. M.; Angeli, C.; Krylov, A. I.; Granovsky, A. A.; et al. Shape of multireference, equation-of-motion coupled-cluster, and density functional theory potential energy surfaces at a conical intersection. *J. Chem. Theory Comput.* **2014**, *10*, 3074–3084.
- (26) Ferré, N.; Filatov, M.; Huix-Rotllant, M.; Adamo, C. *Density-functional methods for excited states*; Springer, 2016; Vol. 368.
- (27) Hait, D.; Head-Gordon, M. Orbital optimized density functional theory for electronic excited states. *J. Phys. Chem. Lett.* **2021**, *12*, 4517–4529.
- (28) Cunha, L. A.; Hait, D.; Kang, R.; Mao, Y.; Head-Gordon, M. Relativistic Orbital-Optimized Density Functional Theory for Accurate Core-Level Spectroscopy. *J. Phys. Chem. Lett.* **2022**, *13*, 3438–3449.
- (29) Li, Z.; Liu, W. Theoretical and numerical assessments of spin-flip time-dependent density functional theory. *J. Chem. Phys.* **2012**, *136*, 024107.
- (30) Wang, F.; Ziegler, T. Time-dependent density functional theory based on a noncollinear formulation of the exchange-correlation potential. *J. Chem. Phys.* **2004**, *121*, 12191–12196.
- (31) Shao, Y.; Head-Gordon, M.; Krylov, A. I. The spin-flip approach within time-dependent density functional theory: Theory and applications to diradicals. *J. Chem. Phys.* **2003**, *118*, 4807–4818.
- (32) Sears, J. S.; Sherrill, C. D.; Krylov, A. I. A spin-complete version of the spin-flip approach to bond breaking: What is the impact of obtaining spin eigenfunctions? *J. Chem. Phys.* **2003**, *118*, 9084–9094.
- (33) Mato, J.; Gordon, M. S. A general spin-complete spin-flip configuration interaction method. *Phys. Chem. Chem. Phys.* **2018**, *20*, 2615–2626.
- (34) Mato, J.; Gordon, M. S. Analytic non-adiabatic couplings for the spin-flip ORMAS method. *Phys. Chem. Chem. Phys.* **2020**, *22*, 1475–1484.
- (35) Casida, M. E. Propagator corrections to adiabatic time-dependent density-functional theory linear response theory. *J. Chem. Phys.* **2005**, *122*, 054111.
- (36) Zhang, X.; Herbert, J. M. Spin-flip, tensor equation-of-motion configuration interaction with a density-functional correction: A spin-complete method for exploring excited-state potential energy surfaces. *J. Chem. Phys.* **2015**, *143*, 234107.
- (37) Lee, S.; Filatov, M.; Lee, S.; Choi, C. H. Eliminating spin-contamination of spin-flip time dependent density functional theory within linear response formalism by the use of zeroth-order mixed-reference (MR) reduced density matrix. *J. Chem. Phys.* **2018**, *149*, 104101.
- (38) Lee, S.; Kim, E. E.; Nakata, H.; Lee, S.; Choi, C. H. Efficient implementations of analytic energy gradient for mixed-reference spin-flip time-dependent density functional theory (MRSF-TDDFT). *J. Chem. Phys.* **2019**, *150*, 184111.
- (39) Hirata, S.; Head-Gordon, M. Time-dependent density functional theory within the Tamm–Dancoff approximation. *Chem. Phys. Lett.* **1999**, *314*, 291–299.
- (40) Horbatenko, Y.; Sadiq, S.; Lee, S.; Filatov, M.; Choi, C. H. Mixed-Reference Spin-Flip Time-Dependent Density Functional Theory (MRSF-TDDFT) as a Simple yet Accurate Method for Diradicals and Diradicaloids. *J. Chem. Theory Comput.* **2021**, *17*, 848–859.
- (41) Lee, S.; Shostak, S.; Filatov, M.; Choi, C. H. Conical Intersections in Organic Molecules: Benchmarking Mixed-Reference Spin-Flip Time-Dependent DFT (MRSF-TD-DFT) vs Spin-Flip TD-DFT. *J. Phys. Chem. A* **2019**, *123*, 6455–6462.
- (42) Park, W.; Shen, J.; Lee, S.; Piecuch, P.; Filatov, M.; Choi, C. H. Internal Conversion between Bright (11Bu+) and Dark (21Ag-) States in s-trans-Butadiene and s-trans-Hexatriene. *J. Phys. Chem. Lett.* **2021**, *12*, 9720–9729.
- (43) Park, W.; Alías-Rodríguez, M.; Cho, D.; Lee, S.; Huix-Rotllant, M.; Choi, C. H. Mixed-reference spin-flip time-dependent density functional theory for accurate x-ray absorption spectroscopy. *J. Chem. Theory Comput.* **2022**, *18*, 6240–6250.
- (44) Komarov, K.; Mironov, V.; Lee, S.; Pham, B. Q.; Gordon, M. S.; Choi, C. H. High-performance strategies for the recent MRSF-TDDFT in GAMESS. *J. Chem. Phys.* **2023**, *158*, 194105.
- (45) Davidson, E. R. The iterative calculation of a few of the low-eigenvalues and corresponding eigenvectors of large real-symmetric matrices. *J. Comput. Phys.* **1975**, *17*, 87–94.
- (46) Open Quantum Platform (OQP) shall be released publicly, which has an efficient code for MRSF-TDDFT. It is written in mostly modern Fortran and C/C++ wrapped by a Python Interface. If you wish to test it or perform collaborative developments, please email us for early access.
- (47) Maeda, S.; Ohno, K.; Morokuma, K. Updated Branching Plane for Finding Conical Intersections without Coupling Derivative Vectors. *J. Chem. Theory Comput.* **2010**, *6*, 1538–1545.
- (48) Nikiforov, A.; Gamez, J. A.; Thiel, W.; Huix-Rotllant, M.; Filatov, M. Assessment of approximate computational methods for conical intersections and branching plane vectors in organic molecules. *J. Chem. Phys.* **2014**, *141*, 124122.
- (49) Domcke, W.; Yarkony, D. R.; Köppel, H., Eds. Conical Intersections. *Electronic Structure, Dynamics and Spectroscopy*; Advanced Series in Physical Chemistry; World Scientific: Singapore, 2004; Vol. 15.
- (50) Robb, M. A. In *Conical Intersections. Theory, Computation and Experiment*; Domcke, W., Yarkony, D. R., Köppel, H., Eds.; Advanced Series in Physical Chemistry; World Scientific: Singapore, 2011; Vol. 17, pp 3–50.
- (51) Teller, E. The Crossing of Potential Surfaces. *J. Phys. Chem.* **1937**, *41*, 109–116.
- (52) Herzberg, G.; Longuet-Higgins, H. C. Intersection of Potential Energy Surfaces in Polyatomic Molecules. *Discuss. Faraday. Soc.* **1963**, *35*, 77–82.
- (53) Longuet-Higgins, H. C. The intersection of potential energy surfaces in polyatomic molecules. *Proc. R. Soc. London Ser. A. Mathematical and Physical Sciences* **1975**, *344*, 147–156.
- (54) Atchity, G. J.; Xantheas, S. S.; Ruedenberg, K. Potential energy surfaces near intersections. *J. Chem. Phys.* **1991**, *95*, 1862–1876.
- (55) Yarkony, D. R. In *Conical Intersections. Electronic Structure, Dynamics and Spectroscopy*; Domcke, W., Yarkony, D. R., Köppel, H., Eds.; Advanced Series in Physical Chemistry; World Scientific: Singapore, 2004; Vol. 15, pp 41–127.
- (56) Migani, A.; Olivucci, M. In *Conical Intersections. Electronic Structure, Dynamics and Spectroscopy*; Domcke, W., Yarkony, D. R., Köppel, H., Eds.; Advanced Series in Physical Chemistry; World Scientific: Singapore, 2004; Vol. 15, pp 271–320.
- (57) Polli, D.; Altoe, P.; Weingart, O.; Spillane, K. M.; Manzoni, C.; Brida, D.; Tomasello, G.; Orlandi, G.; Kukura, P.; Mathies, R. A.; et al. Conical intersection dynamics of the primary photoisomerization event in vision. *Nature* **2010**, *467*, 440–443.
- (58) Tully, J. C. Perspective: Nonadiabatic dynamics theory. *J. Chem. Phys.* **2012**, *137*, 22A301.
- (59) Conyard, J.; Addison, K.; Heisler, I. A.; Cnossen, A.; Browne, W. R.; Feringa, B. L.; Meech, S. R. Ultrafast dynamics in the power stroke of a molecular rotary motor. *Nature Chem.* **2012**, *4*, 547–551.
- (60) Yarkony, D. R. Diabolical Conical Intersections. *Rev. Mod. Phys.* **1996**, *68*, 985–1013.

- (61) Bernardi, F.; Olivucci, M.; Robb, M. A. Potential energy surface crossings in organic photochemistry. *Chem. Soc. Rev.* **1996**, *25*, 321–328.
- (62) Tuna, D.; Lefrançois, D.; Wolanowski, L.; Gozem, S.; Schapiro, I.; Andrúniów, T.; Dreuw, A.; Olivucci, M. Assessment of Approximate Coupled-Cluster and Algebraic-Diagrammatic-Construction Methods for Ground-and Excited-State Reaction Paths and the Conical-Intersection Seam of a Retinal-Chromophore Model. *J. Chem. Theory Comput.* **2015**, *11*, 5758–5781.
- (63) Shavitt, I. In *Modern Theoretical Chemistry Vol. 3: Methods of Electronic Structure Theory*; Schaefer, H. F., III Ed.; Plenum: New York, 1977; pp 189–275.
- (64) Karwowski, J. A.; Shavitt, I. In *Handbook of Mol. Phys. and Quantum Chemistry*; Wilson, S., Ed.; Wiley: Chichester, U.K., 2003; Vol. 2, pp 227–271.
- (65) Szalay, P. G.; Müller, T.; Gidofalvi, G.; Lischka, H.; Shepard, R. Multiconfiguration Self-Consistent Field and Multireference Configuration Interaction Methods and Applications. *Chem. Rev.* **2012**, *112*, 108–181.
- (66) Roos, B. O. In *Ab Initio Methods in Quantum Chemistry II*; Lawley, K. P., Ed.; John Wiley and Sons: New York, 1987; pp 399–446.
- (67) Andersson, K.; Malmqvist, P.; Roos, B. O. Second order perturbation theory with a complete active space self consistent field reference function. *J. Chem. Phys.* **1992**, *96*, 1218–1226.
- (68) Lischka, H.; Dallos, M.; Szalay, P. G.; Yarkony, D. R.; Shepard, R. Analytic evaluation of nonadiabatic coupling terms at the MR-CI level. I. Formalism. *J. Chem. Phys.* **2004**, *120*, 7322–7329.
- (69) Dallos, M.; Lischka, H.; Shepard, R.; Yarkony, D. R.; Szalay, P. G. Analytic evaluation of nonadiabatic coupling terms at the MR-CI level. II. Minima on the crossing seam: Formaldehyde and the photodimerization of ethylene. *J. Chem. Phys.* **2004**, *120*, 7330–7339.
- (70) Karna, S. P.; Yeates, A. T. *Nonlinear optical materials: theory and modeling*; ACS Publications, 1996.
- (71) Marques, M. A. L.; Gross, E. K. U. In *A Primer in Density-Functional Theory*; Fiolhais, C.; Nogueira, F.; Marques, M. A. L., Eds.; *Lecture Notes in Physics*; Springer: Berlin, 2003; Vol. 620, pp 144–184.
- (72) Huix-Rotllant, M.; Nikiforov, A.; Thiel, W.; Filatov, M. In *Density-functional methods for excited states*; Ferré, N.; Filatov, M.; Huix-Rotllant, M., Eds.; *Top. Curr. Chem.*; Springer: Heidelberg, 2016; Vol. 368, pp 445–476.
- (73) Baek, Y. S.; Lee, S.; Filatov, M.; Choi, C. H. Optimization of Three State Conical Intersections by Adaptive Penalty Function Algorithm in Connection with the Mixed-Reference Spin-Flip Time-Dependent Density Functional Theory Method (MRSF-TDDFT). *J. Phys. Chem. A* **2021**, *125*, 1994–2006.
- (74) Pariser, R. Theory of the electronic spectra and structure of the polyacenes and of alternant hydrocarbons. *J. Chem. Phys.* **1956**, *24*, 250–268.
- (75) Bahnicks, D. A. Use of Huckel Molecular Orbital Theory in Interpreting the Visible Spectra of Polymethine Dyes: An Undergraduate Physical Chemistry Experiment. *J. Chem. Educ.* **1994**, *71*, 171.
- (76) Hellmann, H. *Einführung in die Quantenchemie*; Franz Deuticke: Leipzig, 1937; p 285.
- (77) Herndon, W. C.; Silber, E. Simplified molecular orbitals for organic molecules. *J. Chem. Educ.* **1971**, *48*, 502.
- (78) Baker, A. D.; Baker, M. D. A geometric method for determining the Huckel molecular orbital energy levels of open chain, fully conjugated molecules. *J. Chem. Educ.* **1984**, *61*, 770.
- (79) Hudson, B.; Kohler, B. A low-lying weak transition in the polyene α , ω -diphenyloctatetraene. *Chem. Phys. Lett.* **1972**, *14*, 299–304.
- (80) Schulten, K.; Karplus, M. On the origin of a low-lying forbidden transition in polyenes and related molecules. *Chem. Phys. Lett.* **1972**, *14*, 305–309.
- (81) Hudson, B.; Kohler, B. Electronic structure and spectra of finite linear polyenes. *Synth. Met.* **1984**, *9*, 241–253; Proceedings of the Workshop “Synthetic Metals II”.
- (82) Tavan, P.; Schulten, K. The low-lying electronic excitations in long polyenes: A PPP-MRD-CI study. *J. Chem. Phys.* **1986**, *85*, 6602–6609.
- (83) Fuß, W.; Haas, Y.; Zilberg, S. Twin states and conical intersections in linear polyenes. *Chem. Phys.* **2000**, *259*, 273–295.
- (84) Levine, B. G.; Martínez, T. J. Ab initio multiple spawning dynamics of excited butadiene: Role of charge transfer. *J. Phys. Chem. A* **2009**, *113*, 12815–12824.
- (85) Götz, J. P. Vibrational Relaxation in Carotenoids as an Explanation for Their Rapid Optical Properties. *J. Phys. Chem. B* **2019**, *123*, 2203–2209.
- (86) Park, W.; Lee, S.; Huix-Rotllant, M.; Filatov, M.; Choi, C. H. Impact of the Dynamic Electron Correlation on the Unusually Long Excited-State Lifetime of Thymine. *J. Phys. Chem. Lett.* **2021**, *12*, 4339–4346.
- (87) Yamazaki, S.; Taketsugu, T. Nonradiative deactivation mechanisms of uracil, thymine, and 5-fluorouracil: A comparative ab initio study. *J. Phys. Chem. A* **2012**, *116*, 491–503.
- (88) Perun, S.; Sobolewski, A. L.; Domcke, W. Conical intersections in thymine. *J. Phys. Chem. A* **2006**, *110*, 13238–13244.
- (89) Stojanović, L.; Bai, S.; Nagesh, J.; Izmaylov, A.; Crespo-Otero, R.; Lischka, H.; Barbatti, M. New Insights into the State Trapping of UV-Excited Thymine. *Molecules* **2016**, *21*, 1603.
- (90) Hudock, H. R.; Levine, B. G.; Thompson, A. L.; Satzger, H.; Townsend, D.; Gador, N.; Ullrich, S.; Stolow, A.; Martinez, T. J. Ab initio molecular dynamics and time-resolved photoelectron spectroscopy of electronically excited uracil and thymine. *J. Phys. Chem. A* **2007**, *111*, 8500–8508.
- (91) Yu, H.; Sanchez-Rodriguez, J. A.; Pollum, M.; Crespo-Hernández, C. E.; Mai, S.; Marquetand, P.; González, L.; Ullrich, S. Internal conversion and intersystem crossing pathways in UV excited, isolated uracils and their implications in prebiotic chemistry. *Phys. Chem. Chem. Phys.* **2016**, *18*, 20168–20176.
- (92) Kang, H.; Lee, K. T.; Jung, B.; Ko, Y. J.; Kim, S. K. Intrinsic lifetimes of the excited state of DNA and RNA bases. *J. Am. Chem. Soc.* **2002**, *124*, 12958–12959.
- (93) Ullrich, S.; Schultz, T.; Zgierski, M. Z.; Stolow, A. Electronic relaxation dynamics in DNA and RNA bases studied by time-resolved photoelectron spectroscopy. *Phys. Chem. Chem. Phys.* **2004**, *6*, 2796–2801.
- (94) McFarland, B. K.; Farrell, J. P.; Miyabe, S.; Tarantelli, F.; Aguilar, A.; Berrah, N.; Bostedt, C.; Bozek, J. D.; Bucksbaum, P. H.; Castagna, J. C.; et al. Ultrafast X-ray Auger probing of photoexcited molecular dynamics. *Nat. Commun.* **2014**, *5*, 4235.
- (95) González-Vázquez, J.; González, L.; Samoylova, E.; Schultz, T. Thymine relaxation after UV irradiation: the role of tautomerization and $\pi\sigma^*$ states. *Phys. Chem. Chem. Phys.* **2009**, *11*, 3927–3934.
- (96) Gador, N.; Samoylova, E.; Smith, V. R.; Stolow, A.; Rayner, D. M.; Radloff, W.; Hertel, I. V.; Schultz, T. Electronic structure of adenine and thymine base pairs studied by femtosecond electron-ion coincidence spectroscopy. *J. Phys. Chem. A* **2007**, *111*, 11743–11749.
- (97) Canuel, C.; Mons, M.; Piuze, F.; Tardivel, B.; Dimicoli, I.; Elhanine, M. Excited states dynamics of DNA and RNA bases: Characterization of a stepwise deactivation pathway in the gas phase. *J. Chem. Phys.* **2005**, *122*, 074316.
- (98) Samoylova, E.; Schultz, T.; Hertel, I. V.; Radloff, W. Analysis of ultrafast relaxation in photoexcited DNA base pairs of adenine and thymine. *Chem. Phys.* **2008**, *347*, 376–382.
- (99) Ligare, M.; Siouri, F.; Bludsky, O.; Nachtigallova, D.; de Vries, M. S. Characterizing the dark state in thymine and uracil by double resonant spectroscopy and quantum computation. *Phys. Chem. Chem. Phys.* **2015**, *17*, 24336–24341.
- (100) Samoylova, E.; Lippert, H.; Ullrich, S.; Hertel, I. V.; Radloff, W.; Schultz, T. Dynamics of photoinduced processes in adenine and thymine base pairs. *J. Am. Chem. Soc.* **2005**, *127*, 1782–1786.
- (101) Picconi, D.; Barone, V.; Lami, A.; Santoro, F.; Improbato, R. The Interplay between $\pi\pi^*/n\pi^*$ Excited States in Gas-Phase Thymine: A Quantum Dynamical Study. *ChemPhysChem* **2011**, *12*, 1957–1968.
- (102) Szymczak, J. J.; Barbatti, M.; Soo Hoo, J. T.; Adkins, J. A.; Windus, T. L.; Nachtigallova, D.; Lischka, H. Photodynamics simulations of thymine: Relaxation into the first excited singlet state. *J. Phys. Chem. A* **2009**, *113*, 12686–12693.

- (103) Barbatti, M.; Aquino, A. J.; Szymczak, J. J.; Nachtigallová, D.; Hobza, P.; Lischka, H. Relaxation mechanisms of UV-photoexcited DNA and RNA nucleobases. *Proc. Natl. Acad. Sci. U.S.A.* **2010**, *107*, 21453–21458.
- (104) Wolf, T.; Myhre, R. H.; Cryan, J.; Coriani, S.; Squibb, R.; Battistoni, A.; Berrah, N.; Bostedt, C.; Bucksbaum, P.; Coslovich, G.; et al. Probing ultrafast $\pi\pi^*/n\pi^*$ internal conversion in organic chromophores via K-edge resonant absorption. *Nat. Commun.* **2017**, *8*, 29.
- (105) Miura, Y.; Yamamoto, Y.-i.; Karashima, S.; Orimo, N.; Hara, A.; Fukuoka, K.; Ishiyama, T.; Suzuki, T. Formation of Long-Lived Dark States during Electronic Relaxation of Pyrimidine Nucleobases Studied Using Extreme Ultraviolet Time-Resolved Photoelectron Spectroscopy. *J. Am. Chem. Soc.* **2023**, *145*, 3369–3381.
- (106) Kästner, J.; Carr, J. M.; Keal, T. W.; Thiel, W.; Wander, A.; Sherwood, P. DL-FIND: An open-source geometry optimizer for atomistic simulations. *J. Phys. Chem. A* **2009**, *113*, 11856–11865.
- (107) Jónsson, H.; Mills, G.; Jacobsen, K. W. In *Classical and Quantum Dynamics in Condensed Phase Simulations*; Berne, B. J., Ciccotti, G., Coker, D. F., Eds.; World Scientific: Singapore, 1998; Chapter 16, pp 385–404.
- (108) Park, W.; Filatov, M.; Sadiq, S.; Gerasimov, I.; Lee, S.; Joo, T.; Choi, C. H. A Plausible Mechanism of Uracil Photohydration Involves an Unusual Intermediate. *J. Phys. Chem. Lett.* **2022**, *13*, 7072–7080.
- (109) Shostak, S.; Park, W.; Oh, J.; Kim, J.; Lee, S.; Nam, H.; Filatov, M.; Kim, D.; Choi, C. H. Ultrafast excited state aromatization in dihydroazulene. *J. Am. Chem. Soc.* **2023**, *145*, 1638–1648.
- (110) Park, W.; Shen, J.; Lee, S.; Piecuch, P.; Joo, T.; Filatov, M.; Choi, C. H. Dual Fluorescence of Octatetraene Hints at a Novel Type of Singlet-to-Singlet Thermally Activated Delayed Fluorescence Process. *J. Phys. Chem. C* **2022**, *126*, 14976.
- (111) Gilbert, A. T.; Besley, N. A.; Gill, P. M. Self-consistent field calculations of excited states using the maximum overlap method (MOM). *J. Phys. Chem. A* **2008**, *112*, 13164–13171.
- (112) Besley, N. A.; Asmuruf, F. A. Time-dependent density functional theory calculations of the spectroscopy of core electrons. *Phys. Chem. Chem. Phys.* **2010**, *12*, 12024–12039.
- (113) Borden, W. T. In *The Foundations of Physical Organic Chemistry: Fifty Years of the James Flack Norris Award*; Strom, E. T., Mainz, V. V., Eds.; 2015; Vol. 1209, Chapter 11, pp 251–303.
- (114) Abe, M. Diradicals. *Chem. Rev.* **2013**, *113*, 7011–7088.
- (115) Peng, D.; Hu, X.; Devarajan, D.; Ess, D. H.; Johnson, E. R.; Yang, W. Variational fractional-spin density-functional theory for diradicals. *J. Chem. Phys.* **2012**, *137*, 114112.
- (116) Yang, Y.; Peng, D.; Davidson, E. R.; Yang, W. Singlet–triplet energy gaps for diradicals from particle–particle random phase approximation. *J. Phys. Chem. A* **2015**, *119*, 4923–4932.
- (117) Rajca, A. Organic diradicals and polyradicals: from spin coupling to magnetism? *Chem. Rev.* **1994**, *94*, 871–893.
- (118) Gryn'ova, G.; Coote, M. L.; Corminboeuf, C. Theory and practice of uncommon molecular electronic configurations. *WIREs Comput. Mol. Sci.* **2015**, *5*, 440–459.
- (119) Abe, M.; Ye, J.; Mishima, M. The chemistry of localized singlet 1, 3-diradicals (biradicals): from putative intermediates to persistent species and unusual molecules with a π -single bonded character. *Chem. Soc. Rev.* **2012**, *41*, 3808–3820.
- (120) Hund, F. Zur Deutung verwickelter Spektren, insbesondere der Elemente Scandium bis Nickel. *Z. Physik* **1925**, *33*, 345–371.
- (121) Kolc, J.; Michl, J. π -Biradicaloid hydrocarbons. Pleiadene family. I. Photochemical preparation from cyclobutene precursors. *J. Am. Chem. Soc.* **1973**, *95*, 7391–7401.
- (122) Salem, L.; Rowland, C. The Electronic Properties of Diradicals. *Angew. Chem., Int. Ed.* **1972**, *11*, 92–111.
- (123) Gopalakrishna, T. Y.; Zeng, W.; Lu, X.; Wu, J. From open-shell singlet diradicaloids to polyradicaloids. *Chem. Commun.* **2018**, *54*, 2186–2199.
- (124) Komarov, K.; Park, W.; Lee, S.; Zeng, T.; Choi, C. H. Accurate Spin–Orbit Coupling by Relativistic Mixed-Reference Spin-Flip-TDDFT. *J. Chem. Theory Comput.* **2023**, *19*, 953.
- (125) Pomogaev, V.; Lee, S.; Shaik, S.; Filatov, M.; Choi, C. H. Exploring Dyson's orbitals and their electron binding energies for conceptualizing excited states from response methodology. *J. Phys. Chem. Lett.* **2021**, *12*, 9963–9972.
- (126) Huix-Rotllant, M.; Schwinn, K.; Pomogaev, V.; Farmani, M.; Ferré, N.; Lee, S.; Choi, C. H. Photochemistry of thymine in solution and DNA revealed by an electrostatic embedding QM/MM combined with mixed-reference spin-flip TDDFT. *J. Chem. Theory Comput.* **2023**, *19*, 147.
- (127) Schmidt, M. W.; Baldridge, K. K.; Boatz, J. A.; Elbert, S. T.; Gordon, M. S.; Jensen, J. H.; Koseki, S.; Matsunaga, N.; Nguyen, K. A.; Su, S.; et al. General atomic and molecular electronic structure system. *J. Comput. Chem.* **1993**, *14*, 1347–1363.
- (128) Huix-Rotllant, M.; Natarajan, B.; Ipatov, A.; Wawire, C. M.; Deutsch, T.; Casida, M. E. Assessment of noncollinear spin-flip Tamm–Dancoff approximation time-dependent density-functional theory for the photochemical ring-opening of oxirane. *Phys. Chem. Chem. Phys.* **2010**, *12*, 12811–12825.
- (129) Komarov, K.; Park, W.; Lee, S.; Huix-Rotllant, M.; Choi, C. H. Doubly Tuned Exchange–Correlation Functionals for Mixed-Reference Spin-Flip Time-Dependent Density Functional Theory. *ChemRxiv* **2023**, 1.
- (130) Schreiber, M.; Silva-Junior, M. R.; Sauer, S. P.; Thiel, W. Benchmarks for electronically excited states: CASPT2, CC2, CCSD, and CC3. *J. Chem. Phys.* **2008**, *128*, 134110.
- (131) Monino, E.; Loos, P.-F. Spin-conserved and spin-flip optical excitations from the bethe–salpeter equation formalism. *J. Chem. Theory Comput.* **2021**, *17*, 2852–2867.
- (132) Lefrançois, D.; Tuna, D.; Martínez, T. J.; Dreuw, A. The spin-flip variant of the algebraic-diagrammatic construction yields the correct topology of S1/S0 conical intersections. *J. Chem. Theory Comput.* **2017**, *13*, 4436–4441.
- (133) Mato, J.; Gordon, M. S. Analytic Gradients for the Spin-Flip ORMAS-CI Method: Optimizing Minima, Saddle Points, and Conical Intersections. *J. Phys. Chem. A* **2019**, *123*, 1260–1272.
- (134) Slipchenko, L. V.; Krylov, A. I. Spin-conserving and spin-flipping equation-of-motion coupled-cluster method with triple excitations. *J. Chem. Phys.* **2005**, *123*, 084107.
- (135) Pomogaeva, A.; Filatov, M.; Choi, C. H. Manifestations of strong electron correlation in polyacene: Fundamental gap, density of states, and photoconductivity. *Carbon Trends* **2022**, *7*, 100146.